

RADIAL TEMPERATURE PROFILES IN AN AIR ARC

A THESIS

Presented to

The Faculty of the Division of Graduate
Studies and Research

By

Edward Shires

In Partial Fulfillment

of the Requirements for the Degree
Master of Science in Mechanical Engineering

Georgia Institute of Technology

November, 1974

RADIAL TEMPERATURE PROFILES IN AN AIR ARC

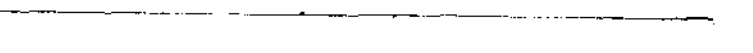
Approved:



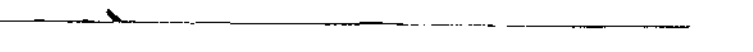
W. Z. Black, Chairman



J. R. Williams



E. Thomas



P. Durbetaki

Date approved by Chairman:

11/11/74

ACKNOWLEDGMENTS

Although the research discussed in this thesis was carried out under the direction of Dr. Uwe H. Bauder and Dr. Ralph S. Devoto, Dr. William Z. Black consented to become the thesis advisor after Drs. Bauder and Devoto left the Mechanical Engineering faculty. The author would like to take this opportunity to thank these men for their help.

Special thanks are also extended to the U. S. Air Force's Arnold Engineering Development Center at Tullahoma, Tennessee, for their financial support of the research.

TABLE OF CONTENTS

	Page
ACKNOWLEDGMENTS.	ii
LIST OF TABLES	v
LIST OF ILLUSTRATIONS.	vi
LIST OF SYMBOLS.	vii
SUMMARY.	x
Chapter	
I. INTRODUCTION.	1
II. THEORY.	3
Total Atomic Line Radiation	
Continuum Radiation	
Molecular Band Radiation	
Side-on Observation	
III. EXPERIMENTAL APPARATUS.	17
IV. EXPERIMENTAL PROCEDURE.	25
Initial Set-up	
Determination of Temperature Profiles from Total	
Atomic Line Radiation	
Determination of Temperature Profiles from	
Continuum Radiation	
Correction for Scattered Light in Continuum and	
Total Atomic Line Lateral Intensity Profiles	
Determination of Temperature Profiles from the	
N ₂ Molecular Band Radiation	
Arc Failure	
V. PRELIMINARY EXPERIMENTS	33
VI. EXPERIMENTS IN AIR.	37
VII. CONCLUDING REMARKS.	45

Appendix	Page
A. DETERMINATION OF THE SCANNING RATE.	49
B. DETERMINATION OF THE RECIPROCAL LINEAR- DISPERSION OF THE SPECTROGRAPH.	50
C. DETERMINATION OF AN APPROXIMATE ATOMIC LINE WIDTH	51
D. DETERMINATION AND USE OF THE SCALE FACTOR . . .	52
BIBLIOGRAPHY	55

LIST OF TABLES

Table		Page
1.	N_2^+ Molecular Constants	12
2.	List of Instruments	22

LIST OF ILLUSTRATIONS

Figure		Page
1.	Total Atomic Line Emission Coefficients of Air. . .	7
2.	N_2^+ Molecular Band Emission Coefficient of Air . .	13
3.	End View of Arc	15
4.	Schematic Diagram of Arc Apparatus.	18
5.	Schematic of Experimental Apparatus	20
6.	Effects of Correction for Scattered Light in Lateral Intensity Profiles upon Radial Temperature Profiles in Argon	30
7.	Radial Temperature Profiles in Argon.	34
8.	Radial Temperature Profiles in Air from Total Atomic Line Radiation at 19, 28, 40, and 80 A . .	38
9.	Radial Temperature Profiles in Air from Total Atomic Line Radiation at 40, 60, and 100 A. . . .	39
10.	Radial Temperature Profiles in Air from N_2^+ Molecular Band Radiation.	40
11.	Proposed Radial Temperature Profiles in Air . . .	41
12.	Comparison of Radial Temperature Profiles in Air and in Nitrogen	42
13.	Axis Temperature Versus Arc Current	43

LIST OF SYMBOLS

A_{mn}	the atomic transition probability from electronic state m to electronic state n (s^{-1})
$A_{N''v''}^{N'v'}$	the band transition probability from the N' electronic and v' vibrational state to the N'' electronic and v'' vibrational state (s^{-1})
A_{PM}	the area of the photomultiplier sensing element (m^2)
c	the speed of light 2.998×10^8 m/s
e	elementary charge 1.6021×10^{-19} J
E	field strength (V/m)
E_m	excitation energy of state m (J)
g_m	the degeneracy of the m electronic state
h	Planck constant 6.624×10^{-34} J·s
i	the absolute intensity of the radiation from the arc ($W/m^3 \cdot sr$)
i_c	the absolute intensity of the continuum radiation ($W/m^3 \cdot sr$)
i_l	the absolute intensity of the atomic line radiation integrated over the width of the atomic line ($W/m^2 \cdot sr$)
i_L	the absolute intensity of the standard lamp ($W/m^3 \cdot sr$)
j	the current from the photomultiplier (A)
j_c	the current from the photomultiplier at the continuum wavelength (A)
j_L	the current from the photomultiplier for the standard lamp intensity (A)
k	Boltzmann constant 1.3804×10^{-23} J/K
K	thermal conductivity (S/m)
K_{PMT}	the photomultiplier sensitivity (A/W)

m	mass of an electron 9.1086×10^{-31} kg
m_o	the magnification of the optical system
n	the number density of the species (m^{-3})
n_e	the number density of electrons (m^{-3})
n_m	the number density in state m of the species (m^{-3})
n_N	the number density of the N_2^+ particles (m^{-3})
n_p	the number of P-form lines viewed
n_R	the number of R-form lines viewed
N	the electronic quantum number
r	distance from center of arc (m)
R	the diameter of the arc (m)
SF_λ	a scale factor ($W/m^3 \cdot sr \cdot A$)
T	the absolute temperature (K)
x	the distance from center of the arc measured normal to the optical axis (m)
y	distance in arc measured along optical axis (m)
Z	the electronic partition function
Z_i	the partition function for the ions
Z_N	the internal partition function for N_2^+
U	total radiation (W/m^3)
γ	the statistical weight of the parent ion
ϵ	emission coefficient ($W/m^4 \cdot sr$)
ϵ_B	the molecular band emission coefficient ($W/m^3 \cdot sr$)
ϵ_L	the total atomic line emission coefficient ($W/m^3 \cdot sr$)
$\epsilon_{\lambda C}$	the continuum emission coefficient ($W/m^4 \cdot sr$)
$\epsilon_{\lambda L}$	the atomic line emission coefficient ($W/m^4 \cdot sr$)
λ	wavelength (m)

λ_{mn}	the center of the wavelengths of the photons given off during the transition from state m to state n (m)
$\Delta\lambda$	wavelength interval (m)
ν	the vibrational quantum number
ξ^{fb}	free-bound factor
ξ^{ff}	free-free factor
σ	electrical conductivity (s)
τ	transmissivity of the optical system
Ω	the solid angle intercepted by the optical system (sr)

SUMMARY

Radial temperature profiles in a steady wall-stabilized direct current electric arc in air at atmospheric pressure were obtained at arc currents of 19, 28, 40, 53, 60, 80, and 100 amperes. Temperatures above 9000 K were determined from the absolute intensity of the total atomic line emission coefficients of the NI 493.5 nm and the OI 436.8 nm atomic lines. The relative intensity of the molecular band emission coefficient of the band head region at 391.4 nm of the $N_2^+ B^2\Sigma_u^+ - X^2\Sigma_g^+ 0,0$ molecular band was used to determine temperatures below 9000 K by the Larenz-Bartels method.

The intensity of the radiation from the arc was measured by a photomultiplier mounted on the exit slit of a spectrograph. Lateral intensity profiles were measured by rotating a mirror such that the image of the arc moved across the entrance slit of the spectrograph. An Abel-inversion computer program converted the lateral intensity profiles to radial emission coefficient profiles.

A preliminary experiment showed that the experimental apparatus and technique produced temperature profiles in argon in agreement with temperature profiles by other researchers. Another preliminary experiment showed that the small flow of air required to keep the electrode shielding gas out of the test section of the arc did not affect the

lateral intensity profiles. Comparison of temperature profiles in argon calculated from a knowledge of the continuum radiation and the total atomic line radiation were in agreement. Since no reported previous work could be found for air at atmospheric pressure, no comparison of temperature profiles in air with other researchers could be made.

CHAPTER I

INTRODUCTION

The topic of this thesis is the experimental determination of the radial temperature profile, $T(r)$, in a steady wall-stabilized electric arc operating in air at atmospheric pressure. Temperature profiles were obtained at several arc currents ranging from 19 to 100 amperes. Temperature was determined from the absolute intensity of the 436.8 nm OI and the 493.5 nm NI total atomic line emission coefficients and the relative intensity of the band head region of the $N_2^+ B^2\Sigma_u^+ - X^2\Sigma_g^+ 0,0$ band near 391.4 nm.

The temperature profile in an electric arc is of little scientific interest by itself but is useful in determining the transport properties of high temperature gases. Using a wall-stabilized direct current electric arc with cylindrical symmetry, Bauder and Maecker [1] explain a technique for determining high temperature gas transport properties, namely: electrical conductivity, $\sigma(T)$; thermal conductivity, $K(T)$; and total radiation, $U(T)$. An important step in their procedure is the determination of the radial temperature profiles. The temperature profiles presented in this thesis were used in determining the transport properties of high temperature (6000 to 14000 K) air at

atmospheric pressure as part of a contract from the U. S. Air Force's Arnold Engineering Development Center at Tullahoma, Tennessee.

Although Maecker and collaborators have determined temperature profiles in argon [2] and in nitrogen [3], the only previously reported determination of temperature profiles in a wall-stabilized electric arc operating in high temperature air at atmospheric pressure was by Schreiber et al. [4] who did not report the current level at which the one temperature profile was reported. Schreiber used a 25.4 mm diameter pulsed arc with electric current pulse durations of up to one second. To prevent oxidation of the electrodes in the electric arc, Schreiber used a nitrogen flow around the electrodes. The nitrogen contaminated the air in the test section however, the presence of nitrogen in the region of the arc was reported to have negligible effects on the temperature profiles. The experimental apparatus (see Chapter III) in this research was a 5 mm diameter wall-stabilized steady electric arc with argon used to shield the electrodes. The argon was not allowed to contaminate the air in the test section.

The purpose of this thesis was to obtain the radial temperature in the arc. The temperature data was to be used by Cailleteau [5] in determining the total radiation and by other researchers in determining the electrical and thermal conductivities.

CHAPTER II

THEORY

The spectrum of radiation given off by a plasma in an electric arc contains molecular bands, atomic and ionic lines, and an electron continuum. All of these spectral phenomena can be used to measure temperature if the relationship between the intensity of the phenomena and the temperature of the plasma can be determined. Using certain simplifying assumptions which will be presented, this chapter will present equations relating temperature and intensity for an atomic line, the electron continuum, and the band head region of a N_2^+ molecular band. The determination of the region of the arc where the radiation was emitted is important since the spatial dependence of temperature in the arc is being determined. This chapter will present a numerical technique used to obtain the radial position in the arc where the radiation was emitted.

The determination of temperature from the intensity of radiation is greatly simplified if one assumes that in the region of the arc being analyzed that the plasma has cylindrical symmetry, the arc operates under conditions of steady state, local thermodynamic equilibrium (L.T.E.) exists, and the plasma is optically thin (negligible

self-absorption) at the wavelengths investigated. Three of the above simplifying assumptions were verified by experimental measurements. Radial symmetry in the plasma was verified by the symmetry of the lateral intensity profiles described in Chapter III. The lack of axial gradients was verified by the constant value of the field strength in the test section of the arc. Field strength was measured using the equipment and procedure described by Cailleteau [5]. Steady state operation of the arc was verified by observing the output of a photocell which viewed the arc and by noting the absence of changes in the photocell's output with time. L.T.E. has also been determined to exist in air plasma in an arc discharge by Gurevich and Podmoshenskii [6]. In determining the temperature in the arc, the assumption of optical thinness is necessary only at the wavelengths where the intensity of the radiation is measured. In air, the 493.5 nm NI and the 436.8 nm OI atomic lines were used to determine temperatures above approximately 9000 K. Below 9000 K, the N_2^+ band head region at 391.4 nm was used as the atomic oxygen and nitrogen particle densities were quite small. Schreiber et al. [4] used the same atomic lines in an air arc and determined that the lines were optically thin in the same temperature range and at the same pressure as this work. The wavelength region of the N_2^+ 391.4 nm band head region was determined by Veneable and Shumaker [7] to be optically thin in an atmospheric nitrogen arc in the same

temperature range as this work. In some preliminary experiments, the arc was used to obtain temperature profiles in argon which required the use of the 430.0 nm AI line. Schulz-Gulde [8] and Morris [9] assure the optical thinness of the argon plasma at 430.0 nm in atmospheric argon arcs.

A final assumption is that only air was present in the test region of the arc. The second preliminary experiment (see Chapter V) assured the argon used for electrode shielding was not present in the test region, and the third preliminary experiment (see Chapter V) assured that tungsten contamination from the electrodes was absent. Spectroscopic analysis showed that no other discernible contaminants were present in the plasma.

Total Atomic Line Radiation

Temperatures above 9000 K in the air arc were determined using the total atomic line radiation. From the detailed analysis of line radiation by Maecker [10], the total atomic line emission coefficient ϵ_L is defined as the energy radiated within one spectral line by a unit volume into unit solid angle per unit time and is given by:

$$\epsilon_L = \frac{1}{4\pi} A_{mn} \frac{hc}{\lambda_{mn}} n_m \quad (\text{W/m}^3 \cdot \text{sr}) \quad (1)$$

where A_{mn} is the atomic transition probability from electronic state m to electronic state n (s^{-1}); λ_{mn} is the center of

the wavelengths of the emitted photons given off during the transition from state m to state n (m); n_m is the number density in state m of the species (m^{-3}); h is Planck constant 6.624×10^{-34} J·s; c is the speed of light 2.998×10^8 m/s. For L.T.E., Boltzmann's relation can be used to determine the number density:

$$n_m = n \frac{g_m}{Z} \exp (-E_m/kT) \quad (m^{-3}) \quad (2)$$

where n is the number density of the species (m^{-3}); k is Boltzmann constant 1.3804×10^{-23} J/K; g_m is the degeneracy of the m electronic state; Z is the electronic partition function; E_m is the excitation energy of state m (J); T is the absolute temperature (K).

Figure 1 shows the total atomic line emission coefficients for the NI 493.5 nm and the OI 436.8 nm lines. The values of the atomic transition probability came from Wiese [11], and the values for the electronic partition function were calculated from atomic constants given in reference [12]. The number densities of atomic oxygen and nitrogen were obtained from Predvoditelev et al. [13,14]. For the preliminary measurements in argon, the total atomic line emission coefficient for the AI 430.0 nm line was obtained from Bauder [15].

The radiation emitted by an atomic transition is not at a unique wavelength; therefore, the atomic line emission

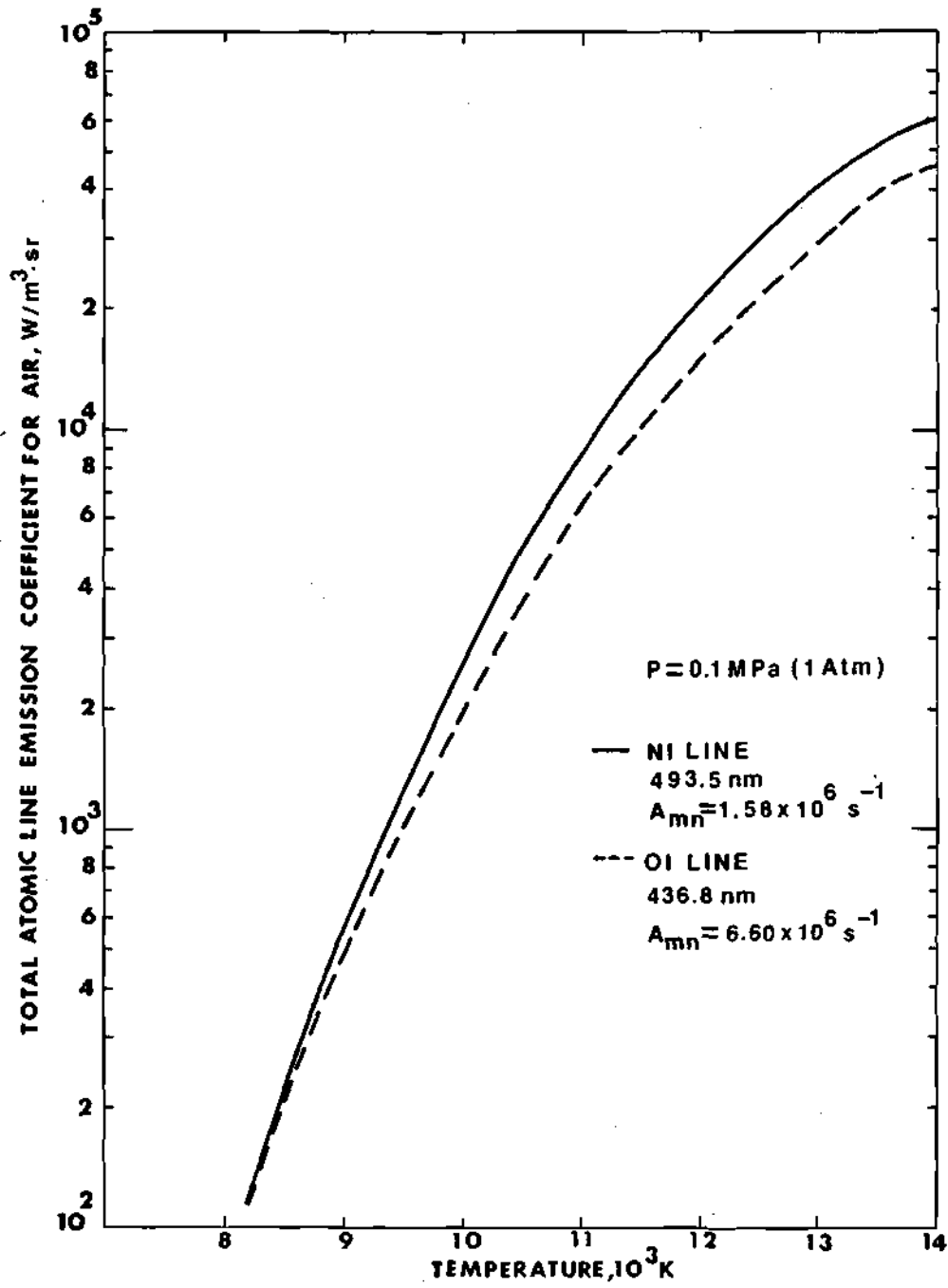


Figure 1. Total Atomic Line Emission Coefficients of Air

coefficient $\epsilon_{\lambda L}$ which is the energy radiated by a unit volume into unit solid angle per unit per unit wavelength is given by

$$\epsilon_{\lambda L} = \frac{1}{4\pi} A_{mn} \frac{hc}{\lambda_{mn}} L(\lambda) \frac{n}{Z} g_m \exp(-E_m/kT) \quad (\text{W/m}^4 \cdot \text{sr}) \quad (3)$$

The $L(\lambda)$ is the line shape factor such that

$$\int_0^{\infty} L(\lambda) d\lambda = 1 \quad (\text{m}) \quad (4)$$

where λ is the wavelength at which the radiation is emitted (m). The line shape factor makes it necessary to intercept a span of wavelength to measure the energy radiated by an atomic transition. The procedure used in this thesis for obtaining the total atomic line radiation is explained in Chapter IV.

Continuum Radiation

Continuum radiation was used only to obtain temperature profiles in argon which was the gas used in the preliminary measurements (see Chapter V). From the Schulz-Gulde [8] analysis of the continuum radiation from an argon arc, the continuum radiation is composed only of free-bound and free-free continuum radiation since the argon plasma does not contain molecules or negative ions.

Free-free continuum radiation occurs when an electron is affected by an ion and passes from a circular orbit to a hyperbolic orbit, i.e. $A^+ + e^- = A^+ + e^- + \text{photon}$. Free-bound radiation occurs when a free electron is captured by an ion, i.e. $A^+ + e^- = A + \text{photon}$. If the argon plasma is in L.T.E. and is optically thin, the continuum emission coefficient $\epsilon_{\lambda C}$ at λ wavelength is given by [8]:

$$\epsilon_{\lambda C} = \frac{8 [2\pi]^{1/2} e^6 n_e^2 \xi(\lambda, T)}{3 [3\text{km}^3]^{1/2} c^2 \lambda^2 [T]^{1/2}} \quad (\text{W/m}^4 \cdot \text{sr}) \quad (5)$$

where n_e is the number density of electrons (m^{-3})

$$\xi(\lambda, T) = \frac{\gamma}{Z_i} \xi^{\text{fb}}(\lambda, T) [1 - \exp(-hc/\lambda kT)] + \quad (6)$$

$$\xi^{\text{ff}}(\lambda, T) \exp(-hc/\lambda kT)$$

Z_i is the partition function of the ions; γ is the statistical weight of the parent ion which for argon $\gamma = 6$; e is the elementary charge 1.6021×10^{-19} J; ξ^{fb} is a free-bound factor first introduced and calculated by Biberman et al. [16] and later refined by Schluter [17]; m is the mass of an electron 9.1086×10^{-31} kg; ξ^{ff} is a free-free factor. Using equations (5) and (6), the continuum emission coefficient for atmospheric argon at 432.0 nm was calculated by

Bauder [18].

Molecular Band Radiation

For the determination of temperatures less than 9000 K in air, the intensity of the radiation given off by a portion of the $N_2^+ B^2\Sigma_u^+ - X^2\Sigma_g^+ 0,0$ band head at 391.4 nm was used. Venable and Shumaker [7] have presented a discussion of the use of a N_2^+ molecular band in determining temperatures in an electric arc and have stated that for a portion of a N_2^+ band head the integrated (over the number of P-form and R-form lines viewed) emission coefficient ϵ_B is given by:

$$\epsilon_B = \frac{1}{4\pi} \frac{n_N}{Z_N} \exp(-\beta[T_e' - G_0(0) + G'(v')]) A_{N''v''}^{N'v'} [\sum_{M'=0}^{n_R} \quad (7)$$

$$[[1 - \frac{[-1]}{3}]^{M'}] [M'+1] \exp(-\beta F'(M')) + \sum_{M'=1}^{n_P} [[1 - \frac{[-1]}{3}]^{M'}]$$

$$[M'] \exp(-\beta F'(M'))]] \quad (W/m^4 \cdot sr)$$

where $\beta = hc/kT$

n_N is the number density of the N_2^+ particles (m^{-3})

Z_N is the internal partition function for N_2^+

$$G(v) = \omega_e [v + \frac{1}{2}] - \omega_e x_e [v + \frac{1}{2}]^2 + \omega_e y_e [v + \frac{1}{2}]^3 \quad (m)$$

$A_{N''v''}^{N'v'}$ is the band transition probability from the

N' electronic and v' vibrational state to the N'' electronic and v'' vibrational state (s^{-1})

$$F'(M') = [-B_e - \alpha_e [\nu + \frac{1}{2}]] M' [M'+1] \quad (m)$$

n_R is the number of R-form lines viewed

n_p is the number of P-form lines viewed

ν is the vibrational quantum number

T_e , α_e , ω_e , $\omega_e x_e$, B_e , and $\omega_e y_e$ are molecular constants and are shown in Table 1 (m).

The single prime indicates the upper level, and the double prime indicates the lower level of the transition. Equation (7) is valid only if L.T.E. exists and if the plasma is optically thin in the band head wavelength region.

Figure 2 shows the integrated emission coefficient for the N_2^+ 391.4 nm band head region (390.55 to 391.4 nm) including P(1) to P(32) (thus $n_p = 32$) and R(0) to R(6) (thus $n_R = 7$) lines. The value of the band transition probability shown was obtained from Venable and Shumaker [7]. The values of the internal partition function were obtained from Drellishak et al. [19], and the N_2^+ number densities were from Liebermann [20]. The N_2^+ 391.4 nm band head radiation results from the $B^2\Sigma_u^+ - X^2\Sigma_g^+$ transition for which the vibrational quantum numbers ν for the upper and lower vibrational states are zero. The molecular constants listed in Table 1 for the upper and lower states are from Wallace [21] and were used in the evaluation of equation (7) in Figure 2.

In $G(\nu)$, the order of magnitude of $\omega_e y_e$ is 10 [22] and thus is negligible compared to the rest of the terms

Table 1. N_2^+ Molecular Constants
(units - cm^{-1})

State	T_e	ω_e	$\omega_e \chi_e$	B_e	α_e
$B^2\Sigma_u^+$	254529	24411	312	20.85	0.25
$X^2\Sigma_g^+$	0.0	22076	169	19.3	0.20

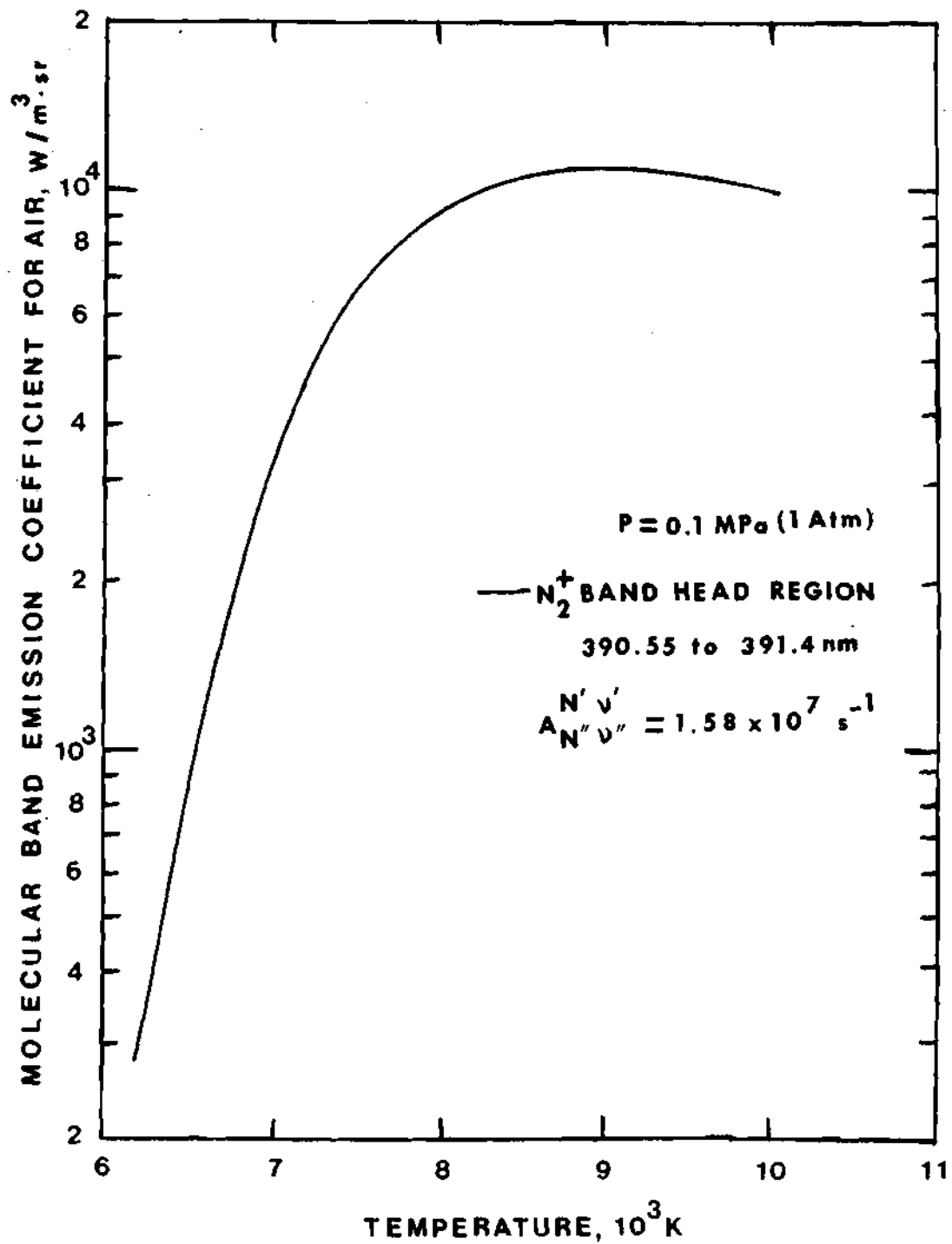


Figure 2. N_2^+ Molecular Band Emission Coefficient of Air

which are of the order of 100 or greater.

One method of determining temperature using molecular band radiation utilizes the fact that a maximum value of the emission coefficient occurs at approximately 9000 K as can be seen in Figure 2. The Larenz-Bartels method as described by Finkelburg and Maecker [23] states that if an off-axis maximum occurs in the observed integrated emission coefficient, the temperature at that point must be 9000 K. Instead of the absolute intensity only some measure of the relative intensity of the observed radiation such as current from the photomultiplier described in Chapter III is required. By assigning the value of the maximum calculated ϵ_B to the maximum off-axis experimental ϵ_B , the experimental ϵ_B can be related to temperature. Venable and Shumaker [7] have presented the argument that for temperatures above 10,000 K the appearance of atomic nitrogen lines in the 391.4 nm band head region significantly affects the band head radiation. The molecular band radiation was thus used only for temperatures below 9000 K in this work.

Side-on-Observation

End-on observation of the arc, that is observing the arc from one electrode toward the other, would be the simplest method to determine the radial emission coefficient profile. Unfortunately, the only way in which to observe the arc end-on is view past the electrodes where the gas

flow causes considerable scattering of the light. Side-on observation was thus used, but viewing the arc from the side presents an additional complication because the light observed at the side comes from different regions of the arc as shown below:

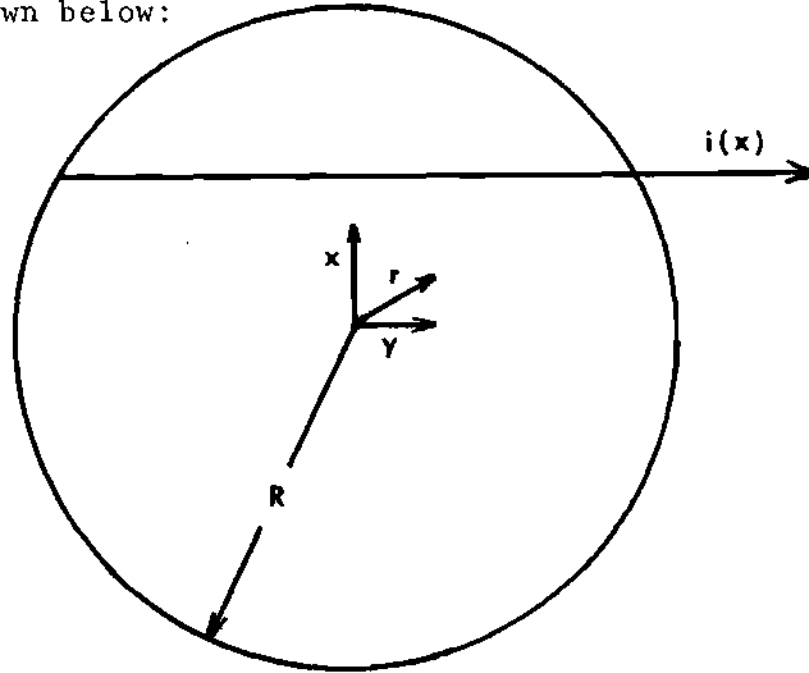


Figure 3. End View of Arc

The lateral intensity profile $i(x)$ is given by:

$$i(x) = 2 \int_0^{(R^2-x^2)^{1/2}} \epsilon(r) dy = 2 \int_x^R \frac{\epsilon(r) r dr}{(r^2-x^2)^{1/2}} \quad (\text{W/m}^2 \cdot \text{sr}) \quad (8)$$

Equation (8) can be used to determine $\epsilon(r)$ after $i(x)$ is measured. The procedure uses an Abel-inversion computer program developed at Aerospace Research Laboratories at Wright-Patterson Air Force Base, Ohio. A lateral intensity

profile of the arc was divided into approximately 40 to 50 points to which the computer program fitted a set of Jacobi polynomials and analytically inverted to obtain $\epsilon(r)$. The output of the program was $\epsilon(r)$ at 0.1 mm increments. One of the input variables of the program was the degree of the polynomial used in the curve-fitting process. This feature of the program is useful since it is well-known [7] that small errors in the intensity measurements near the center of the arc can lead to substantial errors in $\epsilon(r)$ near the origin. To reduce these errors, several polynomials, typically 7th, 9th, and 11th degree, were used; and an average value of $\epsilon(r)$ obtained. The values of $\epsilon(r)$ from the different polynomials agreed to within 10%.

CHAPTER III

EXPERIMENTAL APPARATUS

The experimental apparatus used to generate the wall-stabilized arc was a modification of the apparatus described by Bauder and Stephens [24]. The equipment consisted of four primary systems: an arc apparatus, gas systems, a water cooling system, and equipment to analyze the plasma. The arc apparatus consisted of a cylindrical pressure vessel and a cascade shown schematically in Figure 4. Sixteen copper plates which were 25 mm square, 2 mm thick, and had a 5 mm diameter hole in the center formed the cascade arc constrictor tube. The plates were insulated from each other by 0.3 mm thick silicon rubber washers and were water-cooled continuously through internal passages in the plates. The electrodes were a 5 mm diameter water-cooled thoriated tungsten cathode and a 5 mm thick cascade plate with a tungsten insert as the anode. The cascade was mounted vertically with the cathode at the bottom. The two ports for side-on observation were formed by two cascade plates with optical grade quartz covering the outside of the slits. One side port was used for spectroscopic observation, and the other port was used for total radiation measurements.

To control the pressure in the cascade and to slow

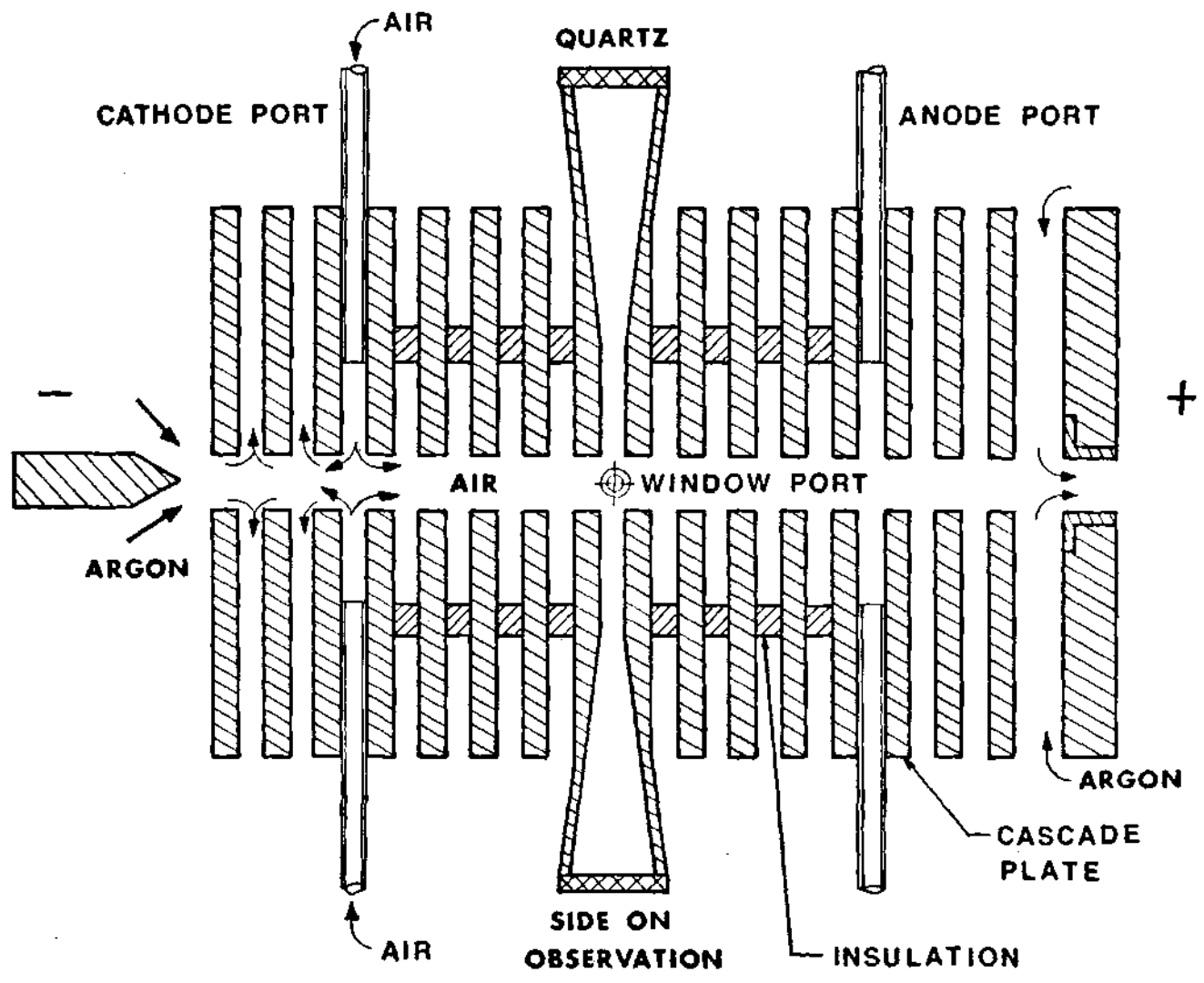


Figure 4. Schematic Diagram of Arc Apparatus

oxidation of the electrodes, the cascade and electrodes were mounted inside a 200 mm diameter cylindrical pressure vessel which is shown schematically in Figure 5. A copper tube (not shown) extended from the inner quartz windows to the outer quartz windows to prevent an interference from the flows in the outer chamber.

The gas systems consisted of two components of which the first controlled the gas (normally air) in the test section. The other component was used to provide gas (normally argon) to shield the electrodes and to pressurize the outer vessel. The test gas was supplied from compressed gas bottles through a regulator to graduated needle valves. It was possible to individually control the flow of the test gas into the cascade through any combination of three positions (see Figure 4): near the cathode, at the observation windows, and near the anode. For measurements in air at atmospheric pressure, only the port near the cathode was used. The shielding and pressure vessel gas also came from gas bottles through a regulator and a needle valve. An exit port on the pressure vessel prevented a build-up of pressure in the pressure vessel during atmospheric operation.

The water cooling system included a 300 kW heat exchanger, a 40 liter per minute positive displacement water pump, and a water purifier. The system was designed to supply the cooling water to the cascade at the static pressure of the test gas thus reducing the stresses in the

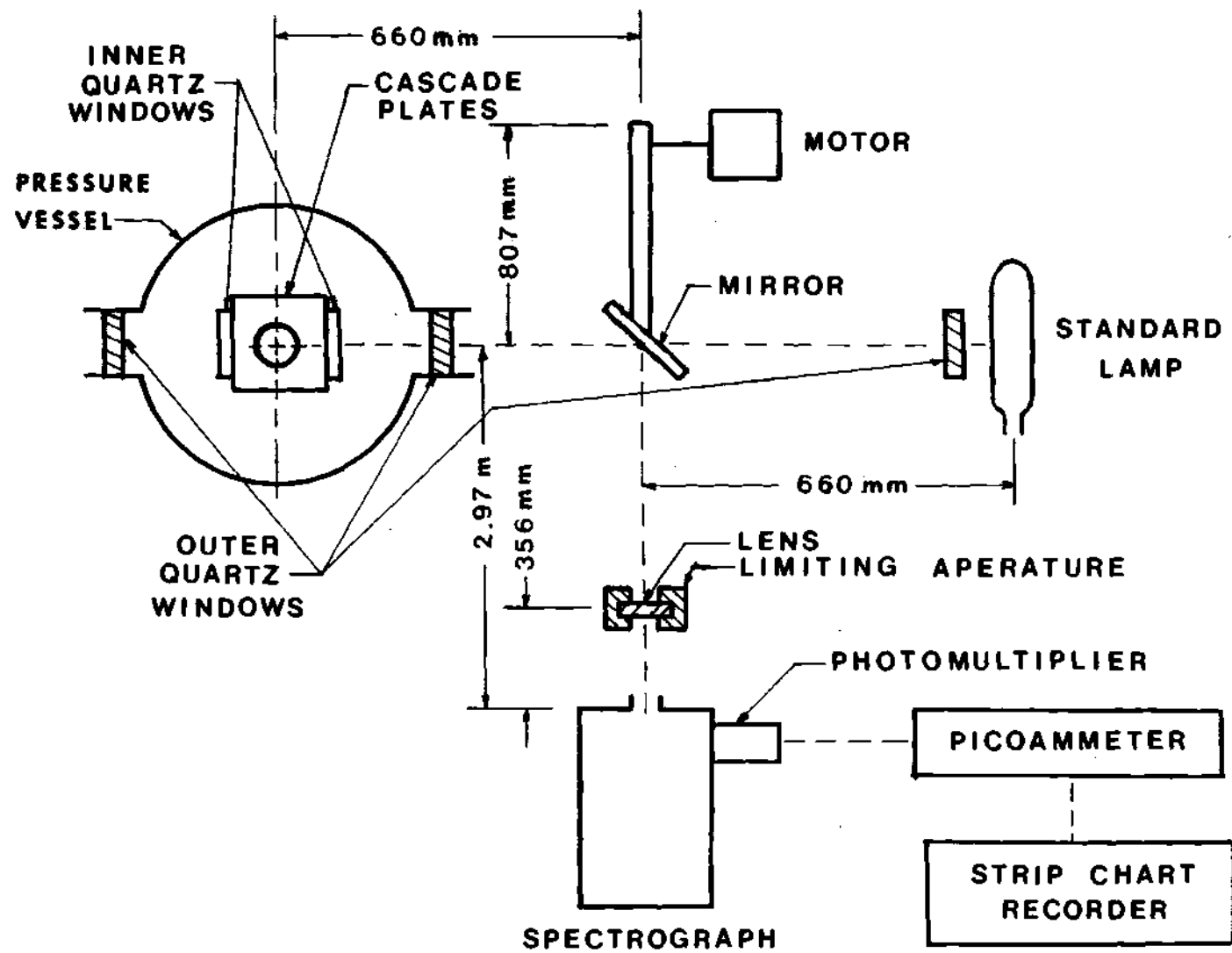


Figure 5. Schematic of Experimental Apparatus

thin-walled cascade plates.

The instrumentation and equipment used to obtain the lateral intensity profiles are shown schematically in Figure 5, and the components are described in Table 2. The apparatus consisted of a rotating mirror to move the image of the arc across the front of the spectrograph; a lens to focus the image; a spectrograph, photomultiplier, picoammeter, and strip chart recorder to measure and record the relative intensity of the radiation; and a standard lamp to obtain the absolute intensity of the radiation.

The high quality mirror was mounted with the axis of rotation passing along the reflecting surface. To make a lateral intensity profile of the arc, the mirror was rotated by an arm which was driven by a reversible synchronous motor through a Gaertner reducer and slide. As the mirror rotated, the image of the arc moved across the entrance slit of the spectrograph at a rate of 0.546 mm of arc width per second (see Appendix A for procedure used to determine the scanning rate). For the spectrograph to view the standard lamp, the mirror was rotated 90 degrees counterclockwise independently of the arm.

The lens imaged the arc on the entrance slit of the McPherson spectrograph which had a linear reciprocal dispersion of 775 picometers per millimeter (see Appendix B for calibration procedure). The entrance slit was opened to give a 20 μm spatial resolution in the arc. An EMI 6255 S

Table 2. List of Instruments

Quartz Windows (Outer)	2.5 mm thick 3.8 mm dia Limiting Aperture = 2.54 mm Index of Refraction \approx 1.52
Quartz Windows (Inner)	5 x 3 x 4 mm
Cascade Plates	2 x 25.15 mm each
Motor and Reducer:	Globe Industries A-C Motor 20 rpm Gaertner Scientific Corporation Reducer and slide.
Mirror:	12.7 x 8.8 mm Pivoted in the center
Standard Lamp:	EG & G Model 590 Calibrated Lamp System 5920 Lamp Housing Calibrated by Epply Laboratories, Inc. Spectral Range of Calibration 250 nm to 750 nm National Bureau of Standards Reference Standards Employed: EU 285 EU 286 EU 289

Table 2 (concluded)

Lens: Karl Lambrecht
Crystal-Quartz-Lithium Floride Achromatic
Objective Lens
Diameter = 32 mm
Focal Length 800+ 50 mm
Chromatic Error \bar{of} .5% or less throughout spectral
range $\lambda = 210.0$ to 600.0 nm

Limiting Aperature: 38 mm outside diameter
29 mm clear

Spectrograph: McPherson

Photomultiplier: EMI 6255S

Picoammeter: Keithley Instruments
Model 416
High speed
Response Time ≈ 4 ms

Strip Chart Recorder: Clevite Brush
Mark 250 Recorder

photomultiplier was placed on the exit slit of the spectrograph to determine the intensity at a certain wavelength. A Keithley picoammeter converted the current output of the photomultiplier to a voltage signal which was recorded using a Clevite-Brush strip chart recorder.

The tungsten-strip standard lamp was part of a EG & G Model 590 Calibrated Lamp System with its calibration traceable to the National Bureau of Standards. To insure the same optical path from the standard lamp as from the cascade, an extra outer quartz window was placed in front of the standard lamp.

CHAPTER IV

EXPERIMENTAL PROCEDURE

The experimental procedure used to determine the radial temperature profiles in an electric arc included: an initial set-up of the experimental apparatus; the determination of the radial temperature profile from the lateral intensity profile using atomic line, continuum, and molecular band radiation; correction for scattered light in the continuum and atomic line lateral intensity profiles; and determination of conditions which led to arc failure.

Initial Set-up

The initial set-up of the experimental apparatus was necessary to insure that the radiation from the arc passed through the quartz windows and the lens without distortion. After leveling all the optical equipment (see Figure 5) on their individual stands, a laser was set up behind the entrance slit of the spectrograph with the laser beam passing through the entrance slit toward the mirror. The lens located between the spectrograph and the mirror was centered in the beam and adjusted until the reflections from the mirror came back along the beam. With the mirror in the position for the spectrograph to view the arc, the cascade and the pressure vessel were adjusted until the laser beam passed through the

centers of the inner and outer quartz windows. The cascade and the pressure vessel were constructed such that the windows would be only a few degrees from perpendicular to the laser beam (necessary to prevent reflections) if the laser beam passed through the centers of the windows. Angling the windows to prevent reflections was also used by Venable and Shumaker [7] in their determination of temperature profiles in nitrogen.

The tungsten-strip standard lamp was positioned with the tungsten strip at the same distance away from the center of the mirror as the distance from the center of the mirror to the center of the cascade. The extra outer quartz window was placed as close as possible to the standard lamp, and the quartz window along with the lamp was adjusted to be on and perpendicular to the optical axis. Measurements showed that rotating the lens a few degrees and moving the standard lamp up and down slightly (\pm approximately 3 mm) had no observable effects on the current output from the photomultiplier.

The arc was then started, and the lens adjusted to give a sharp image on the entrance slit of the spectrograph. The positions of the upper and lower limiting shutters on the entrance slit were adjusted to give a slit height slightly less than the height of the image.

Although the procedures described above were not necessary before each measurement, the alignment of the

equipment was checked at least once during each day's measurements to be sure that none of the equipment was out of adjustment. The rest of the experimental procedure was slightly different depending on whether atomic line, continuum, or molecular band radiation was being measured.

Determination of Temperature Profiles
from Total Atomic Line Radiation

From equations (3) and (4), it can be seen that an atomic line's radiation is dispersed over the entire spectrum. Fortunately $L(\lambda)$ is such that only a negligible amount of energy is given off beyond a few hundred picometers from the center of the line. Appendix C describes the method used to determine an approximate width of a spectral line. The approximate line width was used to set the exit slit of the spectrograph to intercept the total atomic line intensity.

The radiation measured at the atomic line wavelength contains both atomic line radiation and continuum radiation since the processes by which each are formed are independent of each other. Since the intensity of the continuum radiation was found to be constant at wavelengths within ± 3 nm of the wavelength of the line, the continuum radiation at the atomic line wavelength could be removed by using the continuum radiation measured at a nearby line-free wavelength. For the NI 493.5 nm line, the continuum at 495.5 nm was used; and for the OI 436.8 nm line, the continuum at 437.8 nm was

used. In the preliminary measurements in argon, the Al 430.0 nm line and the 432.0 nm continuum were used.

To determine the intensity of the total atomic line radiation, lateral intensity profiles were determined at both the atomic line wavelength and at the continuum wavelength. The standard lamp was used to determine scale factors (see Appendix D) which were used to obtain the absolute intensity at each wavelength. The center of each lateral intensity profile was determined, and the continuum intensity profile subtracted from the continuum plus atomic line intensity profile. The resulting total atomic line lateral intensity profile was then inverted by the Abel-inversion computer program to obtain the radial distribution of the total atomic line emission coefficient. Using the $\epsilon_L(T)$, information contained in Figure 1, radial temperature profiles were obtained.

Determination of Temperature Profiles from Continuum Radiation

The continuum emission coefficient (see equation 5) and the calibration of the standard lamp were both per unit wavelength; therefore, the width of the exit slit of the spectrometer was unimportant as long as no nearby spectral lines were intercepted.

Measurement of the continuum intensity required a lateral intensity profile of the arc at the continuum

wavelength. The standard lamp was used to determine a scale factor (see Appendix D) which in turn was used to obtain a lateral absolute intensity profile. The Abel-inversion program determined $\epsilon_{\lambda C}(r)$ which along with the $\epsilon_{\lambda C}(T)$ information in equation 5 was used to obtain the radial temperature profile in the argon arc.

Correction for Scattered Light in Continuum and Total Atomic Line Lateral Intensity Profiles

The lateral intensity profiles for the continuum or total atomic line radiation showed some scattered light at the edge of the lateral profiles. This observation was also reported by Venable and Shumaker [7]. Removal of this scattered light in the "wings" of the lateral profiles was attempted by using a constant slope approximation after approximately three quarters of the distance from the center of the lateral intensity profile to the edge of the profile. Figure 6 shows that the removal of the wings had negligible effects on a temperature profile in argon.

Determination of Temperature Profiles from the N_2^+ Molecular Band Radiation

The N_2^+ band head at 391.4 nm including the P(1) to P(32) and R(0) to R(6) lines covers the spectral region from 390.55 to 391.4 nm [25]. To intercept the spectral region of the band head, the exit slit on the spectrograph was centered at 391.1 nm and opened to intercept 1.1 nm. The

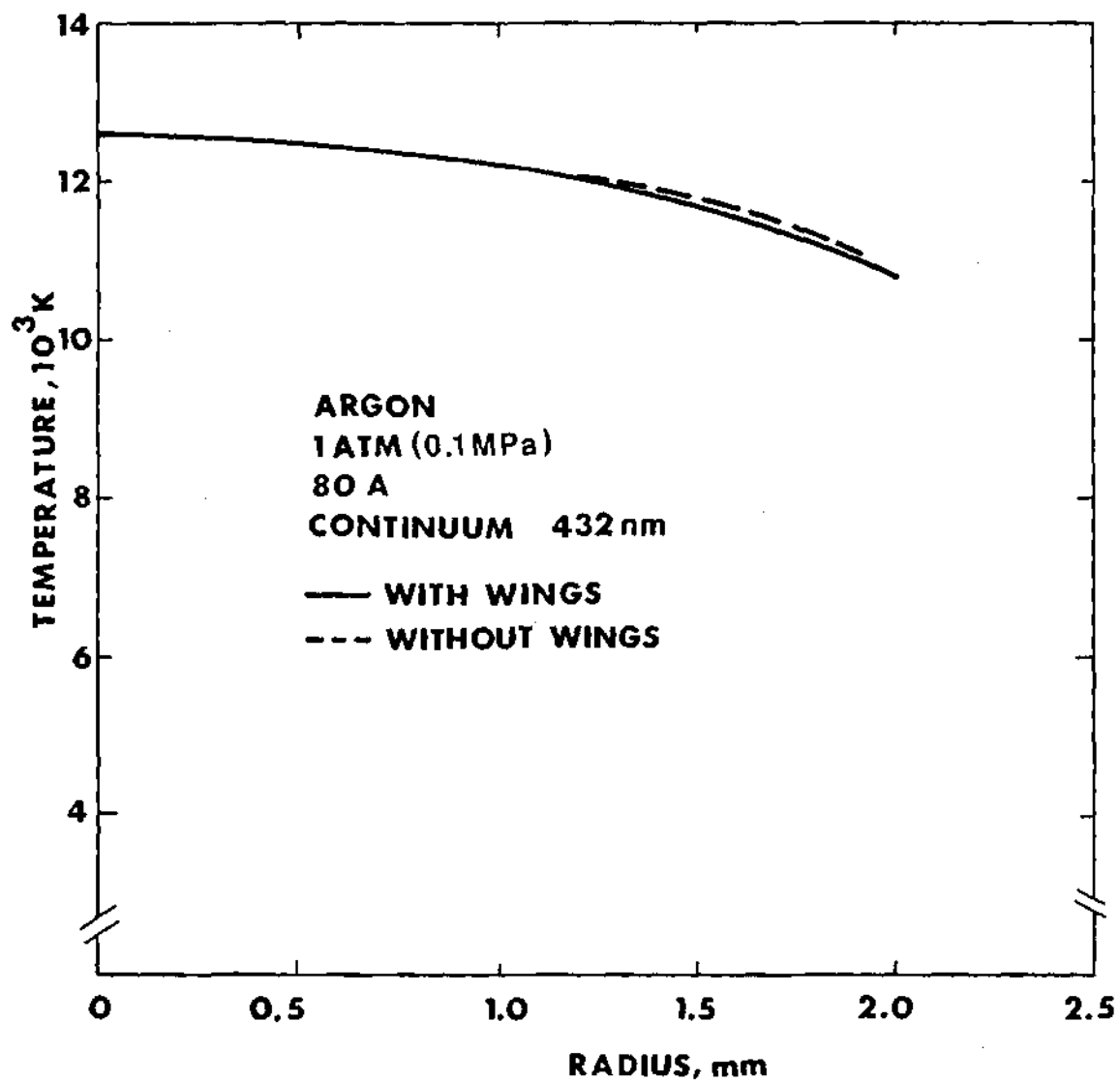


Figure 6. Effects of Correction for Scattered Light in Lateral Intensity Profiles upon Radial Temperature Profiles in Argon

radiation at the band head wavelengths contains both molecular band radiation and continuum radiation since the processes by which each are formed are independent of each other. Since the intensity of the continuum radiation was found to be constant at wavelengths from 391.4 to 394 nm, the continuum radiation at the molecular band head wavelengths could be removed by using the continuum radiation measured at a nearby line-free wavelength, 392.5 nm.

To determine the intensity of the N_2^+ band head, lateral intensity profiles were determined at both the molecular band wavelength and the continuum wavelength. As discussed in Chapter II, the determination of the absolute intensity of the radiation was not necessary. The center of each lateral intensity profile was found, and the continuum intensity profile was subtracted from the continuum plus molecular band intensity profile. The molecular band lateral intensity profile was inverted by the Abel-inversion computer program to obtain the radial distribution of the molecular band emission coefficient. As discussed in Chapter II the off-maximum in the experimental ϵ_B was used to find the absolute intensity of the molecular band emission coefficient. Using the $\epsilon_B(T)$ information contained in Figure 2, the radial temperature profiles were obtained.

Arc Failure

The final portion of the procedure was to observe the

arc to determine when the cascade began to fail. Normally, the cascade failed after five to fifteen minutes in air with little electrode deterioration occurring during operation in argon or nitrogen.

The first mode of failure was when one or more plates burned out thus allowing the cooling water to enter the arc. The image of the arc immediately turned red due to the strong hydrogen lines present.

The second and third modes of failure occurred when the tungsten cathode disintegrated. The tungsten particles were entrained in the flows and deposited on the inner quartz windows. The particles of tungsten also short-circuited the cascade plates, and the short-circuit could be determined from the measurement of the voltage drop per plate which was part of another investigation [5].

CHAPTER V

PRELIMINARY EXPERIMENTS

Four preliminary experiments to test the experimental apparatus and procedures were made before air temperature profiles were determined. The first experiment was to compare temperature profiles in argon with the profiles in the literature. The second experiment was to determine the minimum air flow necessary to prevent the electrode shielding gas from contaminating the air in the test section. The third experiment was to determine the effect of introducing air into the test section. The fourth experiment was to determine whether tungsten vapor was contaminating the air in the test section.

To test the experimental apparatus and procedure for using atomic line radiation to obtain temperature profiles, a preliminary experiment was made in atmospheric argon at 80 amperes. The pressure vessel was filled with argon with no argon introduced into the test section. Two temperature profiles were obtained with one from the continuum radiation at 432 nm and the other from the total atomic line radiation of the AI 430 nm line. The excellent comparison of the two temperature profiles can be seen in Figure 7. It should be noted that the lateral intensity profiles from which the

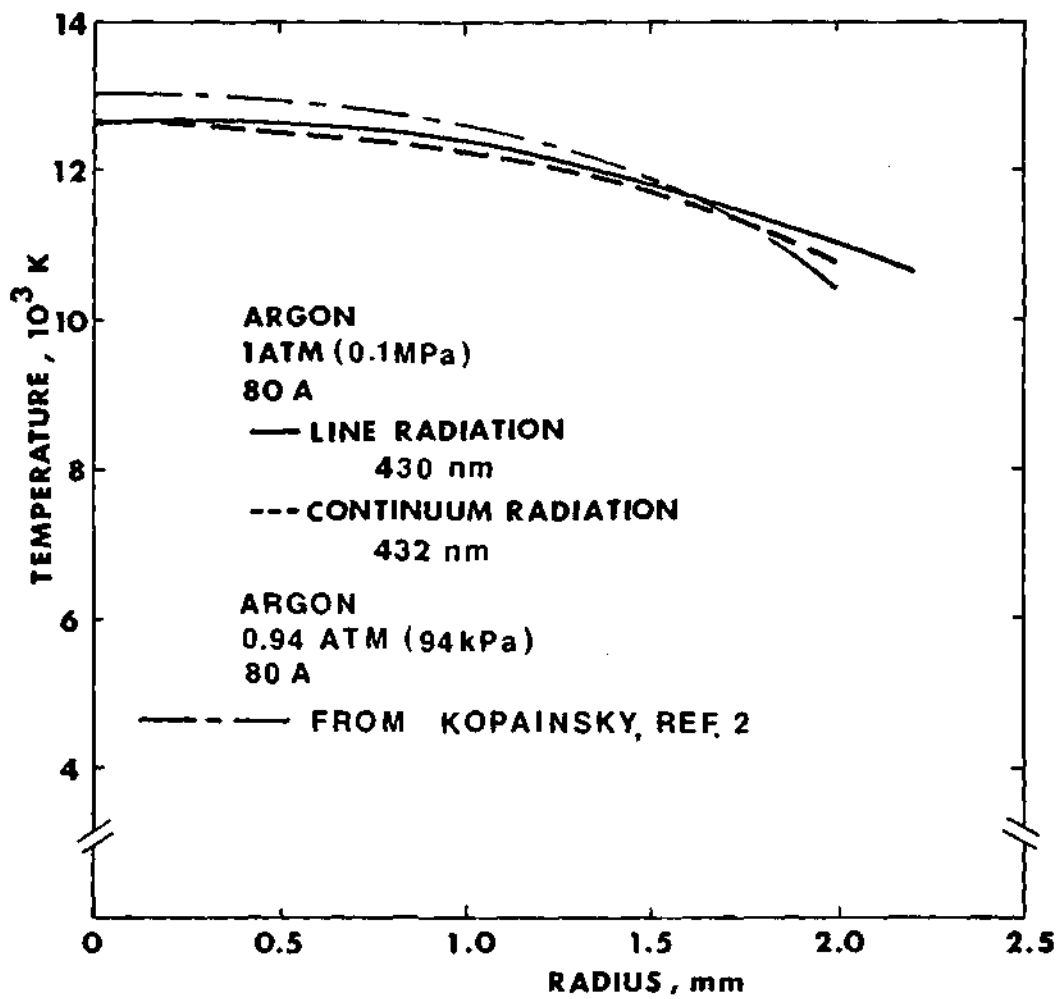


Figure 7. Radial Temperature Profiles in Argon

temperature profiles were calculated were taken several days apart. The good comparison to Kopainsky's [2] 80 ampere temperature profile in argon at 94 kPa (0.94 Atm) is also shown in Figure 7.

The second preliminary experiment was to determine the minimum flow of air necessary to keep the argon gas out of the test section for the air experiments. The arc was started in argon, and the air flow into the port near the cathode (see Figure 4) increased until the presence of the AI 430 line was undetectable above the continuum radiation. The absence of the 425.9, 426.6, 427.2, and 433.3 nm argon lines also proved argon was not present in the test section.

The third preliminary experiment was to determine the effect of introducing a gas into the cascade on the lateral intensity profile. The pressure vessel was filled with nitrogen, and a lateral intensity profile of the NI 493.5 nm line made with no introduction of N_2 into the test section. Another lateral intensity profile was made with N_2 introduced into the test section at the same rate as used for air. The two lateral intensity profiles and the two field strength measurements compared within 3%.

The fourth preliminary experiment was to determine whether tungsten vapor was contaminating the air in the test section of the arc. A spectral scan in the region of the strong tungsten lines at 429.4 and 430.2 nm in the radiation given off by the arc showed that tungsten was either absent

or in such small quantities that it was undetectable in the air.

CHAPTER VI

EXPERIMENTS IN AIR

Using the intensity of the NI 493.5 nm and the OI 436.8 nm atomic lines and a portion of the N_2^+ 391.4 nm band head, radial temperature profiles were obtained in air at atmospheric pressures at arc currents of 19, 28, 40, 53, 60, 80, and 100 amperes. Results are shown in Figures 8, 9, and 10. Figure 11 presents the proposed temperature profiles in the arc which are formed from extrapolating the average of the NI and OI temperature profiles toward the wall and extrapolating the N_2^+ temperature profiles toward the center. Figure 12 presents the comparison between an 80 ampere profile in air and an 80 ampere profile from Schade [3] in nitrogen. The two curves compare favorably considering that air is mostly nitrogen. The curves in Figure 11 exhibit the characteristic of becoming flatter as the current was increased which is a result that Schade has also observed in his work with a nitrogen arc. A plot of the axis temperature as a function of current in Figure 13 exhibits a smooth curve that flattens out with increasing current.

The oxygen line temperature profile is consistently higher than the nitrogen line temperature profile. Schreiber et al. [4] also observed the same characteristic in their

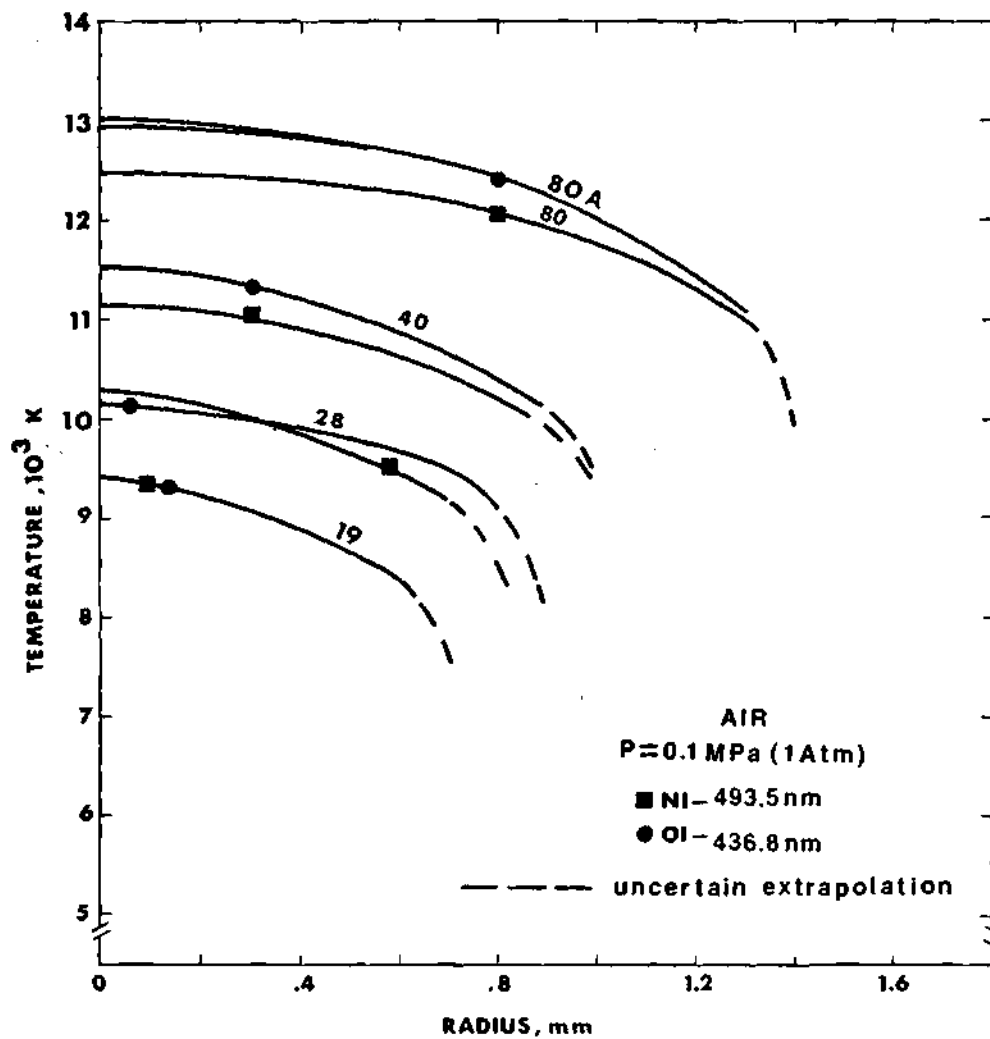


Figure 8. Radial Temperature Profiles in Air from Total Atomic Line Radiation at 19, 28, 40, and 80 A

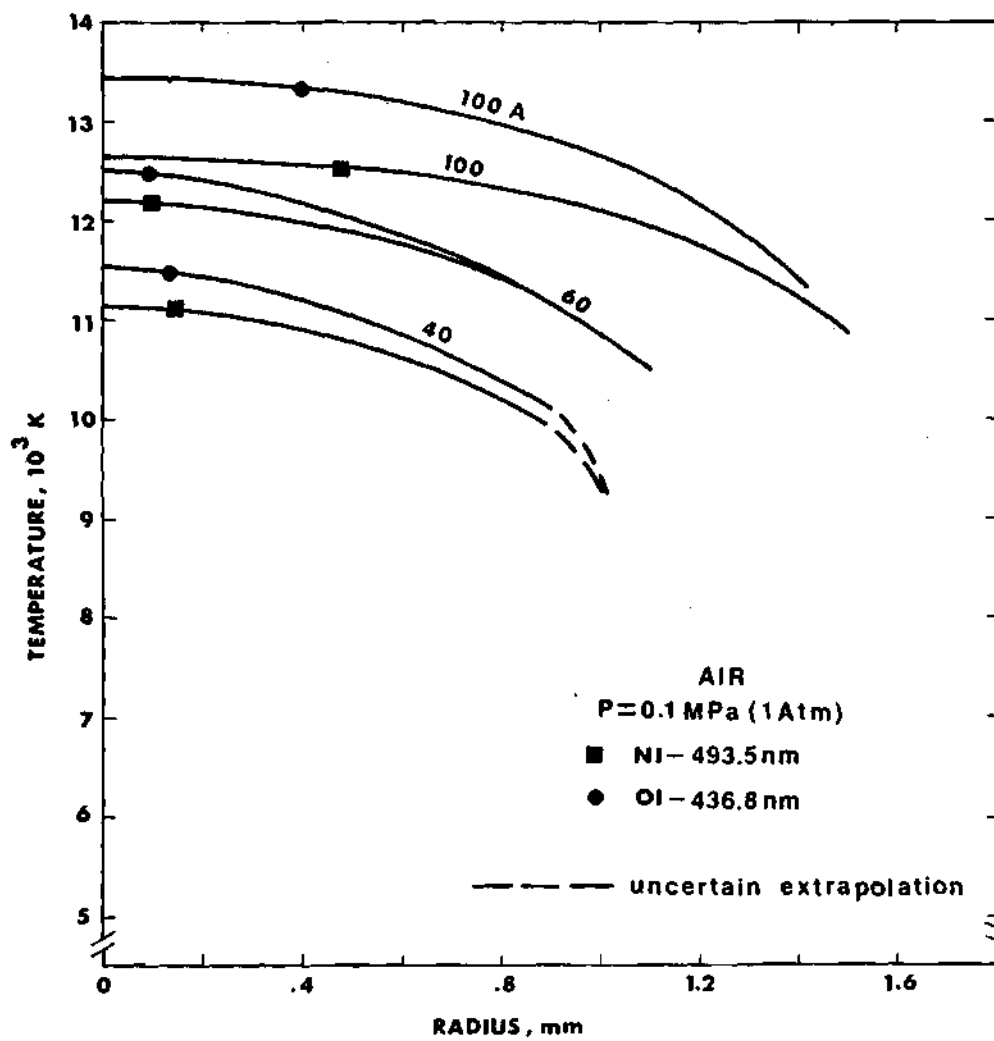


Figure 9. Radial Temperature Profiles in Air from Total Atomic Line Radiation at 40, 60, and 100 A

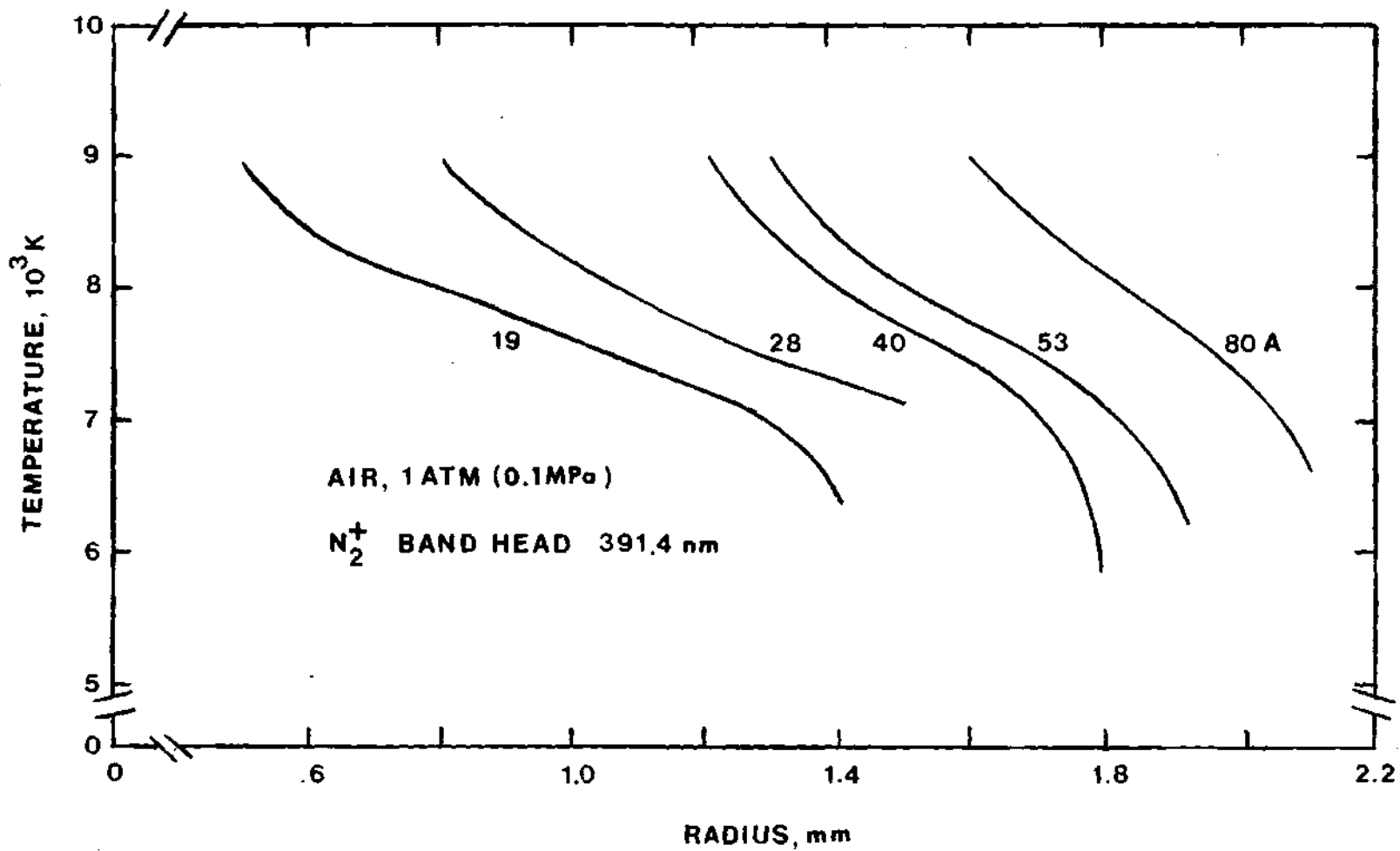


Figure 10. Radial Temperature Profiles in Air from N_2^+ Molecular Band Radiation

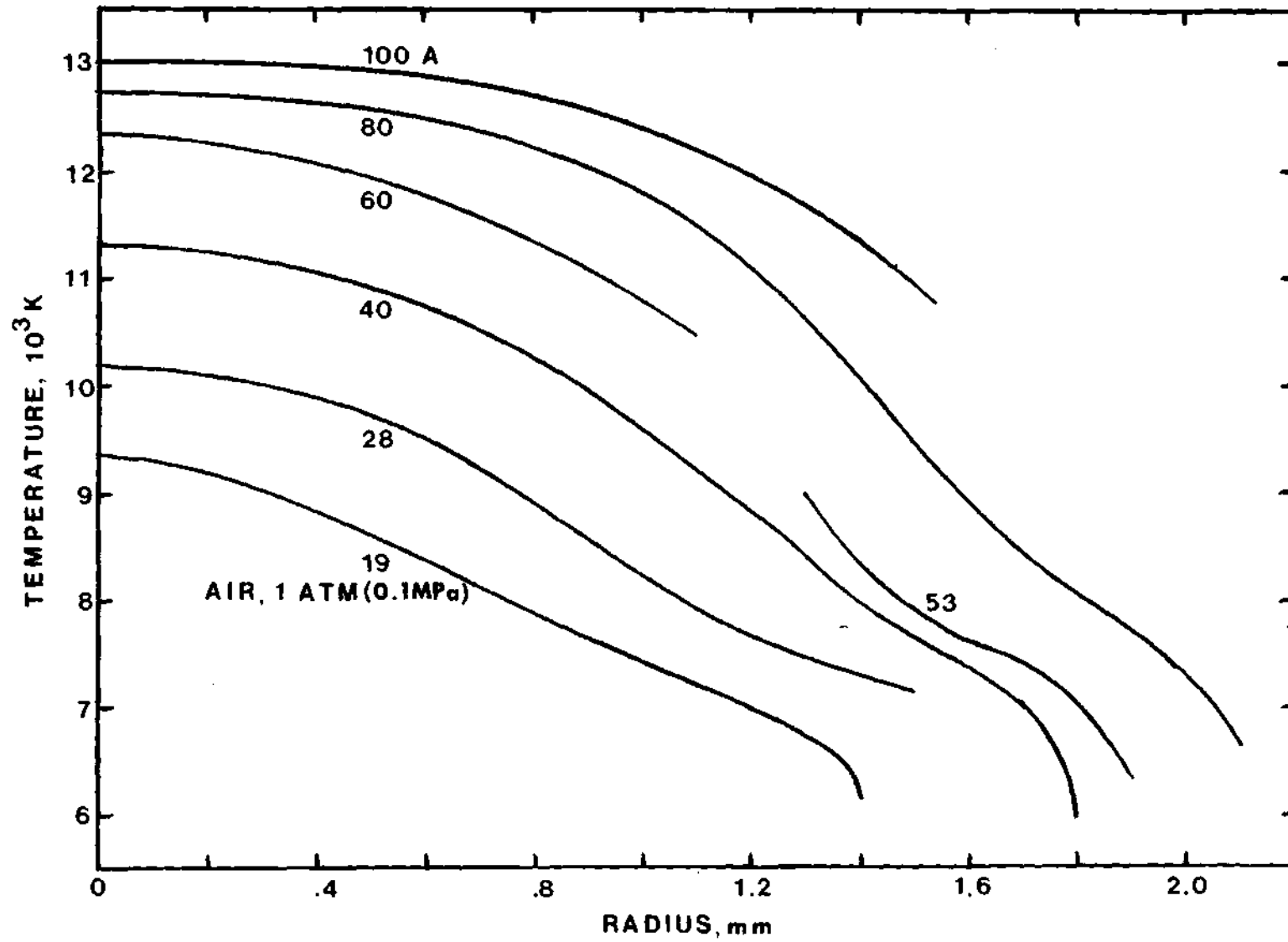


Figure 11. Proposed Radial Temperature Profiles in Air

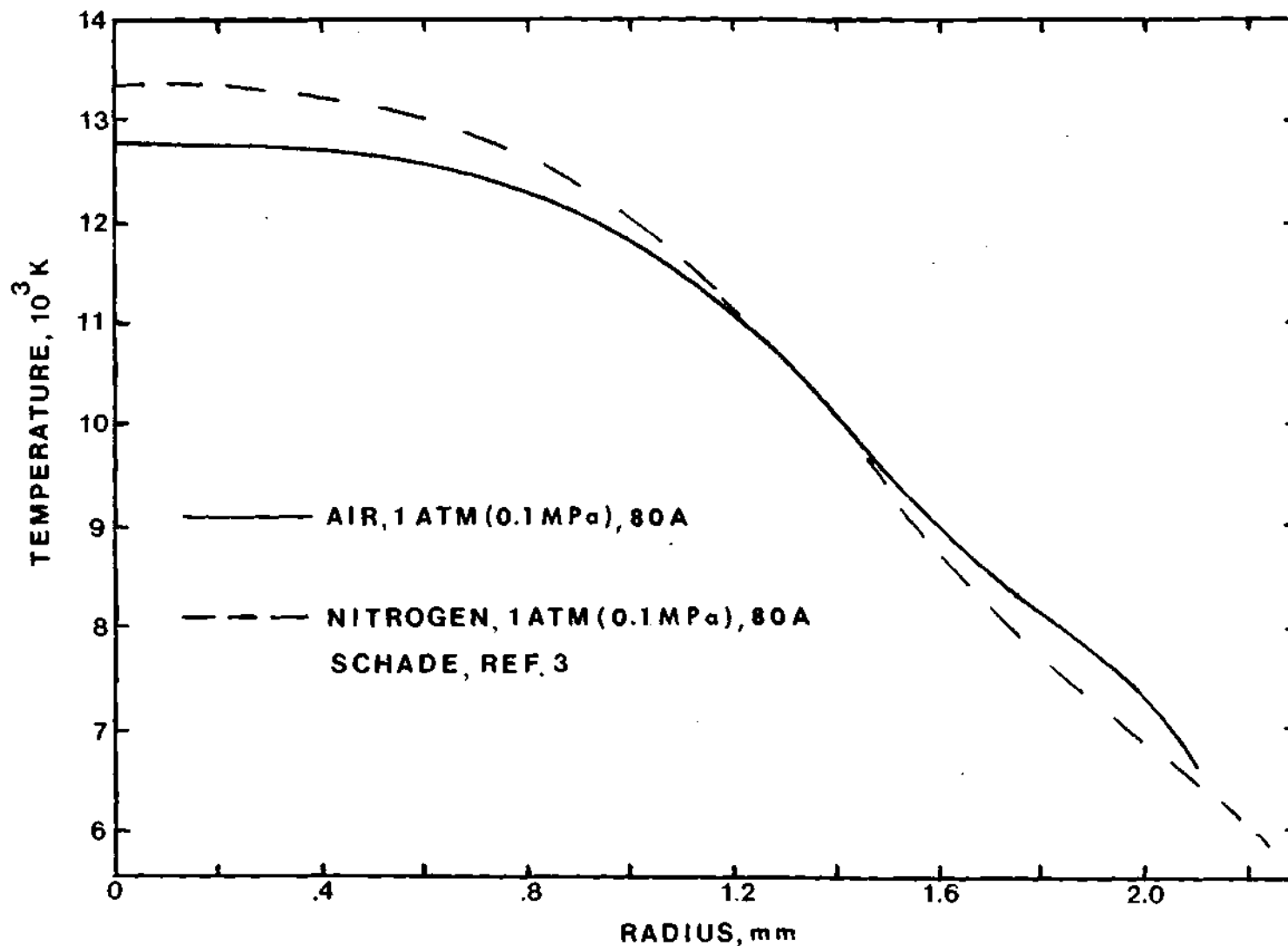


Figure 12. Comparison of Radial Temperature Profiles in Air and in Nitrogen

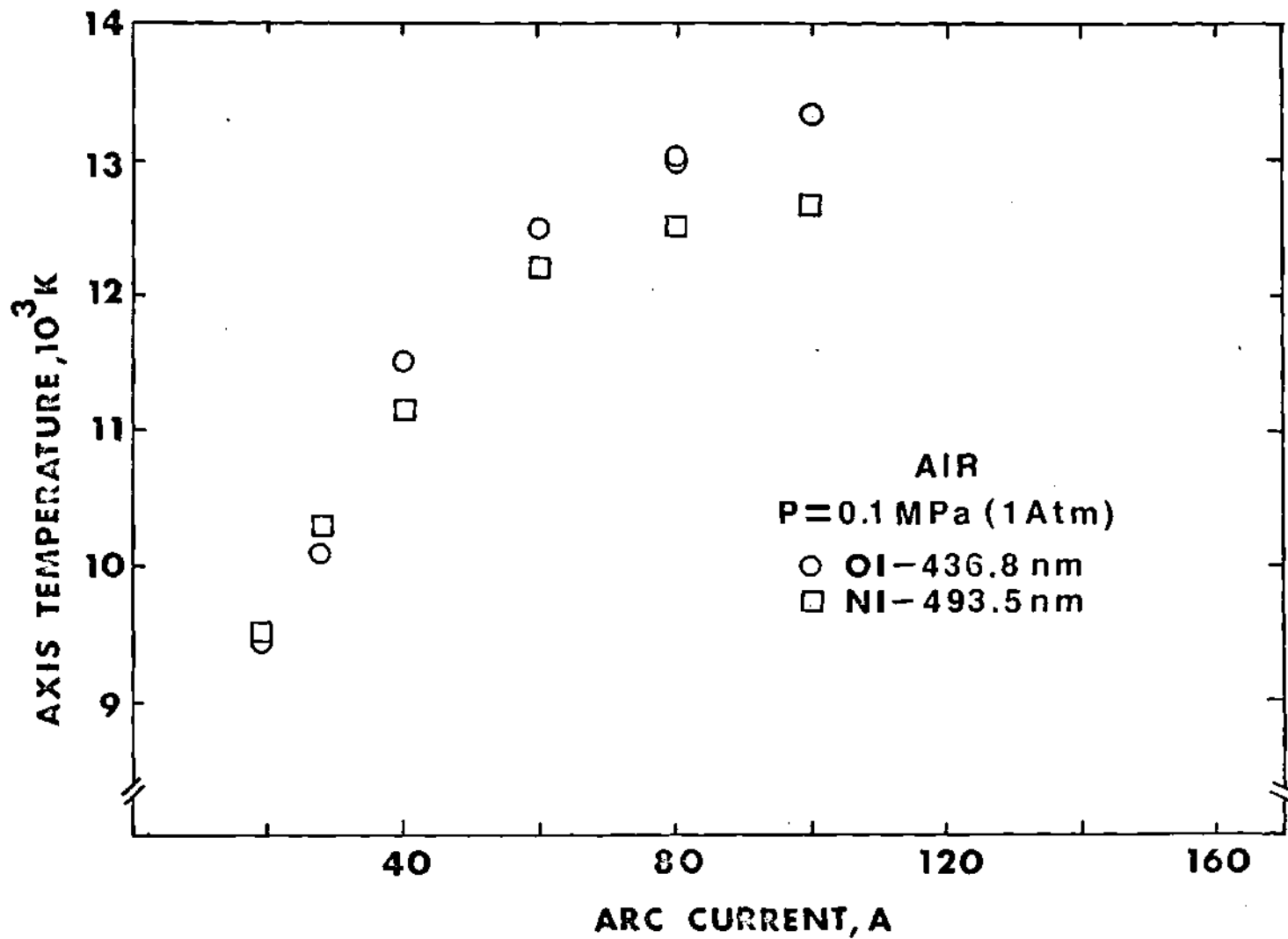


Figure 13. Axis Temperature Versus Arc Current

temperature profile in air.

Estimation of the experimental error is very difficult. The uncertainties in the atomic transition probability of the NI and OI lines are $\pm 10\%$ and $\pm 25\%$, respectively (Reference 14). The band transition probability for the 391.4 nm band head is not very well known [7]. There was approximately 1% error in the measurement of the data, 5% in determining the absolute intensity using the standard lamp, and 5% in the Abel-inversion program. Considering all the sources of error, the error in the temperature profiles should be within 15%. This does not mean that each point in the profile could be $\pm 15\%$ but rather that the entire profile could be moved up and down in temperature by 15%.

CHAPTER VII

CONCLUDING REMARKS

The 80 ampere radial temperature profile in argon at atmospheric pressure determined from the absolute intensity of the total atomic line radiation of the AI 430.0 nm line compared favorably with the 80 ampere temperature profile in argon at atmospheric pressure by Kopainsky [2] as shown in Figure 7. Since Kopainsky had used the same techniques used in this thesis, the experimental apparatus and procedure were demonstrated to produce reliable results for argon. The procedure for determining temperature from the total atomic line radiation was further demonstrated by the excellent comparison between the argon temperature profile determined from the total atomic line radiation and the temperature profile determined from the continuum radiation as shown in Figure 7. When it is noted that the intensity profiles used to calculate the two temperature profiles in argon were made several days apart, at least the partial reproducibility of data was demonstrated. As discussed in Chapter V, the flow and no flow measurements in nitrogen, demonstrated that the lateral intensity profile--and thus the temperature profile--and the field strength were not affected by the introduction of gas into the test section

of the arc cascade. Determination of radial temperature profiles in a steady wall-stabilized direct current arc operating in air in atmospheric pressure using the intensity of the 493.5 nm NI and the 436.8 nm OI atomic lines and the N_2^+ molecular band head at 391.4 nm could thus be assumed to be a reliable method. The favorable comparison between a temperature profile in air and a temperature profile in nitrogen from Schade [3] as shown in Figure 12 also showed the reliability of the temperature profiles in air. The attempt to remove the scattered light from the edges of the lateral intensity profiles as described in Chapter IV showed that scattered light had little effect on a temperature profile in argon as shown in Figure 6.

Due to errors inherent in the Abel-inversion computer program, the radial temperature profiles in air shown in Figures 8, 9, 10, and 11 show unusual trends near the center of the arc and toward the edge of the arc. The curves should be flat at the center, and the curves should not have the almost infinite slopes at the edges. Since the techniques [5] used to determine the temperature dependence of the transport properties do not necessarily require the use of the temperature profiles near the center or at the edge of the arc, these portions of the temperature profiles should not be used.

The average temperature profiles in the arc to be used for determining the transport properties are shown in

Figure 11. Schreiber et al. [4] also used an average temperature profile in their analysis in determining the transport properties.

Recommendations for further work include investigations of higher temperatures in atmospheric air and also measurements at increased pressure. Researchers at Georgia Institute of Technology are presently attempting to operate the same apparatus at pressures up to 3 MPa (30 atm).

APPENDICES

APPENDIX A

DETERMINATION OF THE SCANNING RATE

The determination of the scanning rate was necessary to calculate the position in the arc where the radiation was emitted. The first step in determining the rate at which the image of the arc moved across the entrance slit of the spectrometer was to place a rod of known diameter in the center of the cascade arc with a light shining in from the side opposite the spectroscopic observation port. By knowing the speed (seconds per division) of the strip-chart recorder and the number of divisions between the lighted areas shown on the output, it was determined that the image moved at a rate of 0.546 millimeter of arc width per second. This result was verified to within 1% by an analysis of the linear speed of the Gaertner slide, the distance from the Gaertner slide to the mirror, and the distance from the center of the cascade to the mirror. As the spectrometer views only light that passes through the center of the lens, the magnification has negligible effects.

The distance in the arc that each division on the strip-chart output represented can be calculated from the equation below:

$$\text{distance per division} = 0.546 \frac{\text{mm}}{\text{s}} \times \frac{\text{speed of strip chart}}{\text{in seconds per division}} \quad (9)$$

APPENDIX B

DETERMINATION OF THE RECIPROCAL LINEAR-DISPERSION
OF THE SPECTROMETER

It was necessary to calibrate the spectrometer in the same wavelength region that the measurements were made since the reciprocal linear-dispersion is a weak function of wavelength. The calibration used an arc in argon which produced several prominent atomic lines in the 430 nm region of the spectrum. By adjusting an internal mirror, the spectral dispersion that fell on the exit slit of the spectrometer could also be observed at an opening where a photograph could be made. A photograph was made of the argon spectrum, and the distance between the atomic lines measured using a micro-densitometer. The result was a reciprocal linear-dispersion of 775 picometers per millimeter.

APPENDIX C

DETERMINATION OF AN APPROXIMATE
ATOMIC LINE WIDTH

The determination of an approximate atomic line width was necessary in the experimental procedure for determination of the temperature profiles from total atomic line radiation as described in Chapter IV. The image of the arc was centered on the entrance slit of the spectrometer, and a scan of the spectrum within ± 5 nm of the atomic line wavelength was made with a spectral resolution of 40 pm. The approximate width of the atomic line was measured, and the center of the atomic line located. A nearby line-free region of the spectrum was also located. These measurements resulted in an approximate line width of 775 pm for all the atomic lines used to measure temperature in air and in argon.

APPENDIX D

DETERMINATION AND USE OF THE SCALE FACTOR

From the current output of the photomultiplier, a scale factor was used to determine the absolute intensity of the radiation from the arc. The current j from the photomultiplier is given by:

$$j = i\tau m_o A_{PM}\Delta\lambda K_{PMT}\Omega \quad (A) \quad (10)$$

where

i is the absolute intensity of the radiation from the arc ($W/m^3 \cdot sr$)

τ is the transmissivity of the optical system

m_o is the magnification of the optical system

A_{PM} is the area of the photomultiplier sensing element (m^2)

$\Delta\lambda$ is the wavelength interval (m)

Ω is the solid angle intercepted by the optical system (sr)

K_{PMT} is the photomultiplier sensitivity (A/W)

If a scale factor SF_λ is defined as:

$$SF_\lambda = \frac{i_L}{j_L} = \frac{i_L}{i_L \tau m_o A_{PM} \Delta\lambda \Omega K_{PMT}} = \frac{1}{m_o \tau A_{PM} \Delta\lambda K_{PMT} \Omega} \quad (W/m^3 \cdot sr \cdot A) \quad (11)$$

where

i_L is the absolute intensity of the standard lamp at the wavelength $(W/m^3 \cdot sr)$

j_L is the current from the photomultiplier for the standard lamp intensity (A)

Substituting equation 11 into equation 10 gives:

$$i = j S F_{\lambda} \quad (W/m^3 \cdot sr) \quad (12)$$

Equation 12 can be used for obtaining the absolute intensity of the continuum radiation. For total atomic line and N_2^+ molecular band radiation, a different analysis must be used. Since the radiation at an atomic line or molecular band wavelength contains both continuum radiation and the line or band radiation, it is necessary to remove the continuum radiation to obtain the line or molecular radiation. For example, at the atomic wavelength

$$i \Delta \lambda = i_1 + i_c \Delta \lambda \quad (W/m^2 \cdot sr) \quad (13)$$

where i_1 is the absolute intensity of the atomic line radiation integrated over the wavelength span which is the approximate width of the atomic line $(W/m^2 \cdot sr)$; i_c is the absolute intensity of the continuum radiation $(W/m^3 \cdot sr)$.

From equation 12:

$$i\Delta\lambda = j SF_{\lambda}\Delta\lambda \quad (W/m^2 \cdot sr) \quad (14)$$

and from equation 14 and equation 13:

$$i_1 = j SF_{\lambda}\Delta\lambda - i_c\Delta\lambda \quad (W/m^2 \cdot sr) \quad (15)$$

If the continuum radiation is measured in an adjacent spectral region, the continuum intensity is given by:

$$i_c = j_c SF_{\lambda} \quad (W/m^3 \cdot sr) \quad (16)$$

where j_c is the current from the photomultiplier at the continuum wavelength (A). Multiplying equation 16 by $\Delta\lambda$ and substituting into equation 15 gives:

$$i_1 = j SF_{\lambda}\Delta\lambda - j_c SF_{\lambda}\Delta\lambda \quad (W/m^2 \cdot sr) \quad (17)$$

If the two scale factors are the same

$$i_1 = SF_{\lambda}\Delta\lambda (j - j_c) \quad (W/m^2 \cdot sr) \quad (18)$$

BIBLIOGRAPHY

1. Bauder, U. and H. Maecker, "The Determination of Transport Properties from Arc Experiments: Methods and Results," Proceedings of the IEEE, Vol. 59, 1971, pp. 588-592.
2. Kopainsky, J., "Measurements in Ar High Pressure Arc," Z-Physik, Vol. 248, 1971, pp. 405-416.
3. Schade, E., "Messung von Temperatur Verteilungen in N_2 -Kaskadenbogen bis $26000^\circ K$," Z-Physik, Vol. 233, 1970, pp. 53-64.
4. Schreiber, P. W., A. M. Hunter II, and K. R. Benedetto, "Electrical Conductivity and Total Emission Coefficient of Air Plasma," AIAA Journal, Vol. 11, 1973, pp. 815-821.
5. Cailleateau, J., "Electric Arc Characteristics and Total Radiation from an Air Plasma," M.S. Thesis, School of Mechanical Engineering, Georgia Institute of Technology, 1974.
6. Gurevich, D. B. and I. V. Podmoshenskii, "The Relationship Between the Excitation Temperature and the Gas Temperature in the Positive Column of an Arc Discharge," Optics and Spectroscopy, Vol. 15, 1963, pp. 319-322.
7. Venable, W. H. and J. B. Shumaker, "Observations of Departures from Equilibrium in a Nitrogen Arc," J. Quant. Spectrosc. Radiat. Transfer, Vol. 9, 1969, pp. 1215-1226.
8. Schulz-Gulde, E., "The Continuous Emission of Argon in the Visible Spectral Range," Z.-Physik, Vol. 230, 1970, pp. 449-459.
9. Morris, J. C., R. P. Rudis, and J. M. Yos, "Measurement of Electrical and Thermal Conductivity of Hydrogen, Nitrogen, and Argon at High Temperature," The Physics of Fluids, Vol. 13, 1970, pp. 608-617.
10. Maecker, H., An Introduction to Discharge and Plasma Physics, Department of University Extension, The University of New England, Armidale, N.S.W., Australia.

11. Wiese, W. L., M. W. Smith, and B. M. Glennon, "Atomic Transition Probabilities," U. S. National Bureau of Standards National Standard Reference Data Series 4, Washington, D. C., 1966.
12. "Atomic Energy Levels," National Bureau of Standards Circular 467, Vol. I-III, 1949, 1952, 1958.
13. Predvoditelev, A. S., E. V. Stupochenko, E. V. Samuilov, I. P. Stakhanov, A. S. Pleshanov, and I. B. Rozhdestvenskii, Tables of Thermodynamic Functions of Air for the Temperature Range 6000-12000 K and Pressure Range 0.001-1000 atm, Infosearch Limited, London.
14. Predvoditelev, A. S., E. V. Stupochenko, E. V. Samuilov, I. P. Stakhanov, A. S. Pleshanov, and I. B. Rozhdestvenskii, Tables of Thermodynamic Functions of Air for the Temperature Range 12000-20000 K and Pressure Range 0.001-1000 atm, (original text in Russian).
15. Bauder, U., "Total Atomic Line Emission Coefficient for the AI 430.0 nm Line in an Argon Arc," private communication, Georgia Institute of Technology.
16. Biberman, L. M., G. E. Norman, and K. N. Ulyanov, Optics and Spectroscopy, Vol. 10, 1961, p. 297.
17. Schluter, D., Z-Physik, Vol. 210, 1968, p. 80.
18. Bauder, U., "Continuum Emission Coefficient at 432.0 nm in an Argon Arc," private communication, Georgia Institute of Technology.
19. Drellishak, K. S., D. P. Aeschliman, and Ali-Bulent Camel, "Tables of Thermodynamic Properties of A, N, and O Plasma," AEDC-TDR-64-12, Arnold Engineering Development Center AFSC, USAF, January, 1964.
20. Liebermann, R. W., private communication, Westinghouse Research Labs, Pittsburgh, Pa.
21. Wallace, L., "A Collection of the Band head Wavelengths of N_2 and N_2^+ ," Astrophysics, J. Supplement No. 62, Vol. 6, 1962, pp. 445-480.
22. Herzberg, G., Spectra of Diatomic Molecules (2nd edition), Van Nostrand, Princeton, New Jersey, 1950.
23. Finkelburg, W. and H. Maecker, "Elektrische Bogen and Thermisches Plasma," Handbuch der Physik, Vol. 22.

24. Bauder, U. and E. Stephens, "An Apparatus to Investigate Plasmas at Very High Pressure," The Review of Scientific Instruments, Vol. 43, 1972, pp. 1341-1344.
25. Devoto, R. S., private communication, Georgia Institute of Technology.